Design and Optimization of Interior Permanent Magnet (IPM) Motor for Electric Vehicle Applications

Lavanya Balasubramanian, Nurul Azim Bhuiyan, Asad Javied, Ashraf A. Fahmy, Fawzi Belblidia, and Johann Sienz

***Abstract*—This paper explores some design parameters of an interior permanent magnet synchronous motor that contribute to enhancing motor performance. Various geometry parameters such as magnet dimension, machine diameter, stator teeth height, and number of poles are analyzed to compare overall torque, power, and torque ripples in order to select the best design parameters and their ranges. Pyleecan, an open-source software, is used to design and optimize the motor for electric vehicle applications. Following optimization with Non-dominated Sorting Genetic Algorithm (NSGA-II), two designs A and B were obtained for two objective functions and the corresponding torque ripples values of the design A and B were later reduced by 32% and 77%. Additionally, the impact of different magnet grades on the output performances is analyzed.**

***Index Terms*—Electric vehicles, IPM motor, Magnet grade, Optimization, Permanent magnet motor, Torque ripple.**

I. Introduction

ELECTRIC vehicles (EVs) are a key technology in the frontier of next-generation mobility for meeting global emission reduction targets such as those set out in the Paris Agreement [1] and the targets of the European Union (EU) [2]. The European Union (EU) established a relationship between air quality and automobile emissions in the late 1970s, resulting in enforcing new laws to minimize pollution. The Euro criterion for passenger vehicles was enacted in 1992, and it established a pollution concentration ceiling [3]. With time, these standards become stricter [4], forcing industry to adopt more efficient vehicle powertrains. This may be seen in the growing market share of Hybrid Electric Vehicles (HEVs) and the expected increase in sales over the next decade [5]. Compared to classic Internal Combustion Engines (ICE), electric motors used in EVs are significantly more efficient, with peak efficiency of a typical electrical machine for these applications oscillating around 95%. Additionally, Battery Electric Vehicles (BEVs), in comparison to classic ICE vehicles, are fairly simple and easy to operate as they possess fewer moving parts and a simpler powertrain architecture than a conventional gasoline- powered vehicle. Electric Vehicles consist of only a high voltage battery, an electric motor with a power electronics controller, and a single speed gearbox. Optimization of the powertrain is considered one of the most viable solutions in the automotive industry to reduce the environmental impacts of urban mobility, improve air quality, and achieve emissions targets. The transition towards electrification of vehicles plays a crucial role in creating a greener and more sustainable future. For fuel economy and environment, electric vehicles provide a significant advantage over ICEs and are set to replace the latter in the near future.

Major requirements for electric vehicle motors are high torque and power densities, and widespread operating range, as well as producing low-cost solutions through materials and mass manufacturing capabilities. Permanent Magnet Synchronous Motors (PMSM) are a suitable choice for electric vehicle applications as they provide good performance in terms of high power density and high efficiency [6].

One of the undesirable effects in interior permanent magnet synchronous motor operation is known as the cogging torque [7]. The interaction between the stator teeth and rotor magnets, and the permeance variations during the magnet rotation lead to the production of cogging torque, which eventually lead to audible noise, vibration, fluctuation in speed, and the introduction of torque ripples. In terms of motion control applications, these torque ripples result in signification deterioration of the motor performance and therefore, it is an important aspect to be addressed.

Multiple parameters have been identified in the literature [8] - [11] to have an influence on torque ripples including slot pole combination [12], stator slot opening, slot width, slot height, notch radius [13], airgap length [14], stack length, pole numbers, magnet dimensions, magnet shape and position.

Various studies have explored this issue, and it is understood that one of the most common methods of combating this is by magnet skewing with surface mounted magnets [7], [15]. Magnet skewing involves dividing the magnet into layers and

Manuscript received April 29, 2022; revised August 11, 2022; accepted October 11, 2022. Date of publication June 25, 2023; Date of current version May 31, 2023.

This work was funded by the Advanced Sustainable Manufacturing Technologies (ASTUTE2020) operation supporting manufacturing companies across Wales, which has been part-funded by the European Regional Development Fund through the Welsh Government and the participating Higher Education Institutions. *(Corresponding Author: Lavanya Balasubramanian)*

The authors are with the Advanced Sustainable Manufacturing Technologies (ASTUTE 2020) operation, Swansea University, UK. (e-mail: l.balasubramanian@swansea.ac.uk)

Ashraf A. Fahmy is also with the Department of Electrical Power and Machines, Helwan University, Helwan 11795, Egypt.

Digital Object Identifier 10.30941/CESTEMS.2023.00021

placing them in the rotor in different radial positions that vary by a small angle [16]. The major disadvantage of this method is that it increases cost and manufacturing complexity. Another method of skewing is the stator skewing. However, this complicates automatic winding, and it is not widely popular in mass manufacturing environments.

In order to address the issue of torque ripples, an alternative solution has been proposed by optimizing parameters such as number of poles, magnet dimension, stator teeth height, and stator diameter.

The main purpose of this paper is to identify the best component sizing for a given set of requirements and to attain optimum torque, power, and torque ripples for improved overall electric vehicle performance. It also examines the validity of a new Open-Source software called Pyleecan to analyze the motor characteristics, design and optimization. This paper investigates the tradeoffs between objectives of maximizing torque and minimizing torque ripples, ensuring that the 'best possible' physical motor parameters are selected through optimization. The paper ends with a discussion of the advantages and disadvantages of the optimized designs, along with the effect of different magnet grades.

This work adopted the Tesla Model 3 motor [17] as a baseline design and employs NSGA-II optimization to investigate the trade-offs between two different objective functions of maximizing torque and minimizing torque ripples. Sensitivity analysis is performed to identify the right parameters to optimize. Additionally, the impact of different magnet grades on output performances are analyzed.

II. Methodology

In this section, an electromagnetic model of the internal permanent magnet motor is analyzed, following which, the Pyleecan software is used to verify this model. As discussed previously, the goal is to combat the issue of torque ripples and improve the overall torque, which is first dealt through identification of parameters that influence this by means of a sensitivity analysis. This also provides a starting point for the optimization which has been detailed below. In addition to optimization, a brief overview of the usage of different magnet grades has also been carried out.

A. Electromagnetic Model

The Interior Permanent Magnet Synchronous Machine (IPMSM) motor is modelled analytically in the steady state. The magnetic properties of the chosen magnet materials are given in [18]. A 54 slot 6 pole internal permanent magnet motor based on the Tesla Model 3 motor is designed analytically in MATLAB and verified using Pyleecan software. Magnets are placed in "V" layout and other initial motor specifications for baseline design are given in Table I.

The voltage equations in steady state for direct and quadrature axes of an IPMSM are given by Equations (1) and (2) [19].

$$v_q = R_s i_q + w_e \lambda_m + w_e L_d i_d \quad (1)$$

$$v_d = R_s i_d - w_e L_q i_q \quad (2)$$

where v_q, v_d, i_q, i_d are q and d axis voltages and currents, L_q, L_d are q and d axis inductance. R_s is phase resistance, w_e is electrical frequency, and λ_m is permanent magnet flux linkage. The electromagnetic torque developed for an IPMSM motor can also be found as [19].

TABLE I
MOTOR SPECIFICATIONS [17]

Parameters	Value
Slot-Pole	54-6
Stack Length	135mm
Stator Outer Diameter	116.05mm
Stator Inner Diameter	75.75mm
Rotor Outer Diameter	74mm
Rotor Inner Diameter	35mm
Airgap	0.85mm
Magnet material	N40UH
Rated current	800A
Rated speed	17900RPM

$$T_e = \frac{3p}{2}\left[\lambda_m i_q + \left(L_d - L_q\right)\right] i_d i_q \quad (3)$$

where, p is the number of pole pairs.

B. Pyleecan Model

Analytical model is verified using Pyleecan (Python Library for Electrical Engineering Computational Analysis). It is a Python-based open-source software that includes object-oriented modelling of 2D radial flux machines, multi-objective optimization, and output data visualisation [20]. The motor used in this paper was handled in this software by means of its Graphical User Interface, in which, the motor design parameters were defined in their respective sections. This motor was then simulated using the magnetic and electrical modules in the software to observe the performance in terms of electromagnetic torque, torque ripples, and output power. The air gap flux density of the Pyleecan model was observed as 1.5T from the output result of the electromagnetic model and it differs by only 3% from the analytical design, which gives good validity of the model. The baseline data of analysis and design was adopted from the Tesla Model 3 motor [17]. Fig. 1 shows the Pyleecan model developed.

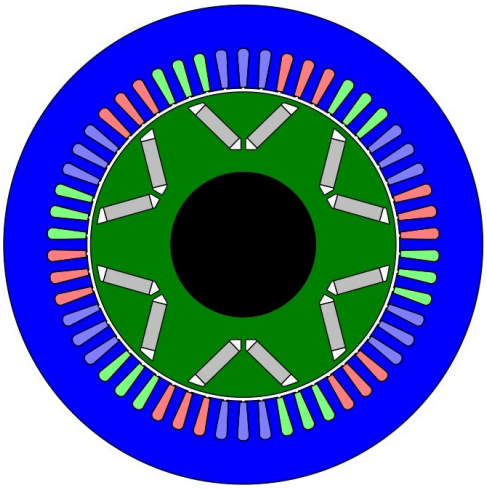

Fig. 1. Tesla Model 3 motor design in Pyleecan.

The overall torque of the above simulated motor is 402 Nm and the power is 167 kW. Fig. 2 shows the output of the above

simulated motor. It can be observed that there is a high fluctuation in torque of 30.57 Nm, which is the torque ripples peak to peak value.

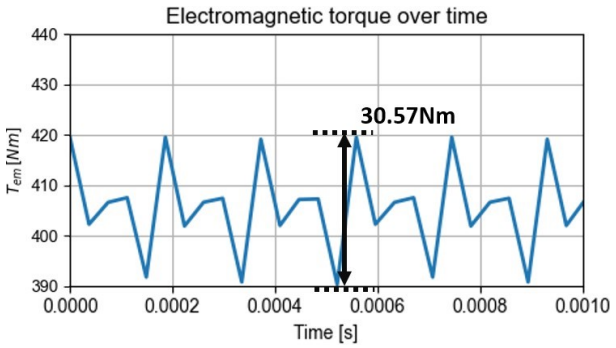

Fig. 2. Motor output with observed torque ripples.

C. Sensitivity Analysis

Our sensitivity analysis considers some parameters chosen from the literature: magnet dimensions, pole number, stator teeth height, and stator outer diameter. The effect of these parameters on overall torque and torque ripples are described in more detail below.

1) Effect of magnet dimensions: In order to identify expected behaviour and choose the right parameters to optimize, an individual sensitivity analysis was carried out. It is known that the permanent magnets in the motor have an impact on the overall motor performance [21]. Therefore, the effect of magnet dimensions on torque and torque ripples were studied to achieve the desired performance.

For this analysis, the magnet height was varied from 15 mm to 25 mm. The values of torque and torque ripples for these magnet heights are shown in Fig. 3. It can be observed that as the magnet height increases, the torque increases linearly, and the torque ripples vary non-linearly. The highest magnet height feasible for this design is 25 mm, which gives a torque fluctuation of nearly 30 Nm. At 15 mm height, the torque ripples drop to 18 Nm but, it is accompanied by a 26% reduction in torque.

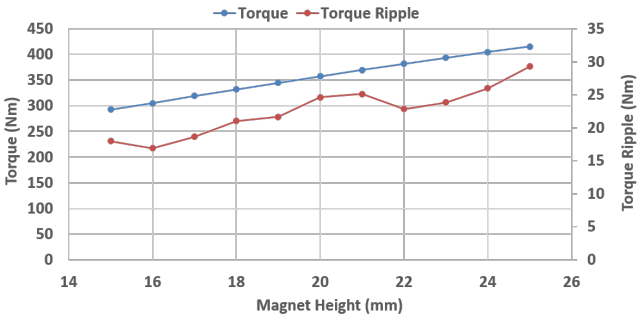

Fig. 3. Effect of magnet height on torque and torque ripples.

Fig. 4 shows the effect of varying the magnet width on torque and torque ripples. With an increase in magnet width, there is an increase in both torque and torque ripples. These two individual sensitivity analyses show that maximum torque is achieved at the largest height and width of the magnet. To identify the values that improve torque with low ripples, these two parameters were chosen for optimization.

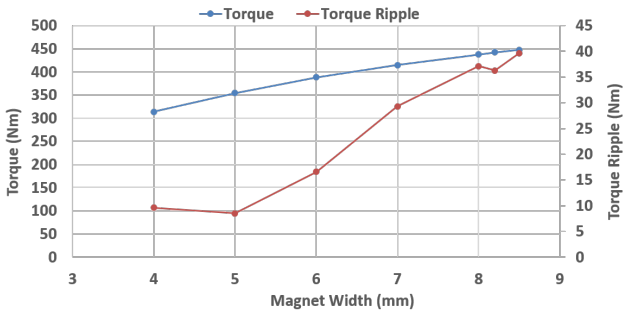

Fig. 4. Effect of magnet width on torque and torque ripples.

2) Effect of Pole number: Fig. 5 demonstrates the variation in torque and torque ripples based on the number of poles in the motor while the slots are constant. Increasing the pole from 6 to 8 results in a drop in torque ripples value. This variation is because of the increase in the value of the least common multiple of slot and pole number [22]. Further increase in pole number reduces the torque below the desired value. Through this analysis, only 6 poles and 8 poles provided the desired ranges and were used for the optimization process.

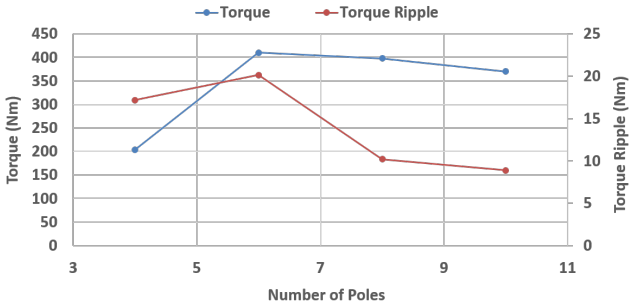

Fig. 5. Effect of pole number of torque and torque ripples.

3) Effect of stator teeth height: The stator teeth height was varied from 15 mm to 30 mm, and the effect of this variation on torque and torque ripples are seen in Fig. 6. In this case, as the teeth height increases, the torque is observed to gradually decrease from about 410 Nm to 300 Nm, and the torque ripples have a sinusoidal variation with the highest value at 30 Nm and lowest at 17 Nm. There is also a local minimum of 18 Nm, which can be identified through convex optimization.

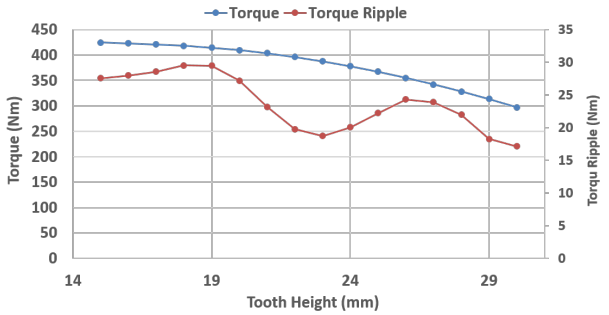

Fig. 6. Effect of teeth height on torque and torque ripples.

4) Effect of stator outer diameter: For this analysis, the stator outer diameter was varied from 115 mm to 120 mm, and the effect of this variation is shown in Fig. 7. It can be observed that larger outer diameter of stator results in increased torque as well as minimal reduction in torque ripples, which stabilize from 119 mm onward.

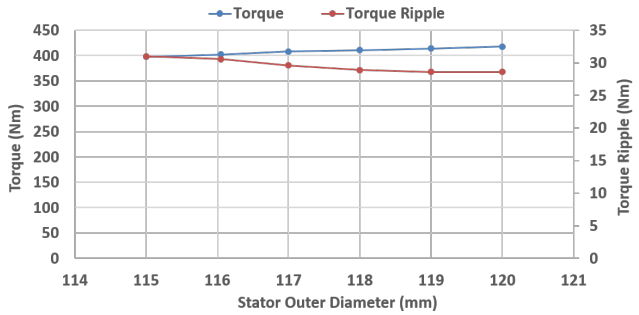

Fig. 7. Effect of stator outer diameter on torque and torque ripples.

D. Optimization

The Pyleecan software utilise the NSGA-II algorithm [23] for the multi-objective optimization. It is one of the most efficient algorithms in the realm of multi-objective optimizations and is particularly suitable for this problem due to its speed and accuracy. In this method, a random initial population is generated, and the goal is to narrow down designs that meet the objective of the optimization and rank them. From that population, the offspring are generated through selection, crossover, and mutation. This process repeats until the algorithm terminates [24]. In terms of solutions, the genetic algorithm does not converge to a single value and instead generates a Pareto solution set of multiple values reflecting trade-offs between competing objectives [25], [26]. This process is followed by human decision to choose the best trade-off among the solution set and, thereby, the optimal solution for the problem [27].

As defined in [28], the optimization problem can be written as

$$\begin{cases} \min \boldsymbol{f}_1(X) \\ \max \boldsymbol{f}_2(X) \\ \boldsymbol{X}_i^{(l)} < \boldsymbol{X}_i < \boldsymbol{X}_i^{(u)} \end{cases} \quad (4)$$

where, $\boldsymbol{f}_1$ is the torque ripples and $\boldsymbol{f}_2$ is the torque average. These form a vector of objective function which depend on a vector of design variables $\boldsymbol{X}$ = ($\boldsymbol{X}_1$, $\boldsymbol{X}_2$,..., $\boldsymbol{X}_n$) and i=1,...,D where D is the boundary constraints.

In this case, design variables such as magnet height, magnet width, stator teeth height, pole number, and stator diameter were considered, while the design constraints such as air-gap clearance, limiting maximum flux density to avoid saturation in stator and rotor yoke, and limiting maximum rotor speed were applied. The population size was set as 52 and the generation number as 8 for reasonable convergence time. The optimization range of the values shown in Table II were decided based on the feasibility of the design and the sensitivity analysis.

E. Different Magnet Grades

The impact of different magnet grades on the output performances were analyzed by replacing baseline magnet grade N40UH with different magnet grade of same temperature range. Table III shows different Neodymium magnet grades that were used for this analysis.

TABLE II
OPTIMIZATION RESULTS

	Input Parameters					Output Parameters		
	Magnet Width (mm)	Magnet Length (mm)	Stator Outer Diameter (mm)	Stator Teeth Height (mm)	Pole Number	Torque (Nm)	Torque Ripples (Nm)	Power (kW)
Initial	7	25	116.05	18.8	6	402	30.57	167
Range	4 to 8.5	15 to 25	115 to 120	15 to 30	6 or 8			
Optimal A	8	24	117	19.2	6	417	20.74	173
Optimal B	7	22	120	22	8	380	6.88	148

TABLE III
DIFFERENT MAGNET GRADES

Magnet grade	Remanent flux density(T)
N30UH	1.13
N35UH	1.21
N40UH	1.29
N42UH	1.31

III. RESULTS

A. Optimization

Table II consists of the design parameters and results of the optimization process. The initial design produced a torque of 402 Nm with 30 Nm torque ripples and 167 kW output power. Following optimization, there were two designs for the desired objectives. With design A, it can be seen that it is possible for a small reduction in torque ripples and an increase in torque and power by increasing magnet width, stator diameter, teeth height and reducing magnet length while maintaining the number of poles. Whereas, design B has increased pole number, stator diameter, teeth height and reduced magnet length while magnet width is maintained. This results in a significantly reduced torque ripples, but it is accompanied by a small reduction in torque and power.

Following optimization, the algorithm converges to a set of solutions in the lower left section as shown in the pareto front in Fig. 8. Here, the arrow points to the chosen design A which has the best trade-off between torque and torque ripple values. The torque and torque ripples of design A is shown in Fig. 9. It can be seen that the torque is 417 Nm which is a 3.5% increase from the initial design and the maximum torque ripple is 20.74 Nm which is a 32% decrease from the initial design.

Fig. 10 shows the torque and torque ripples of the design B. In this design, the torque is 380 Nm, which is a 5.5% decrease from the initial design. However, the torque ripples can be observed to be reduced by 77% to 6.88 Nm. Fig. 11 shows the pareto front obtained from this optimization in which, the arrow points to the chosen design B.

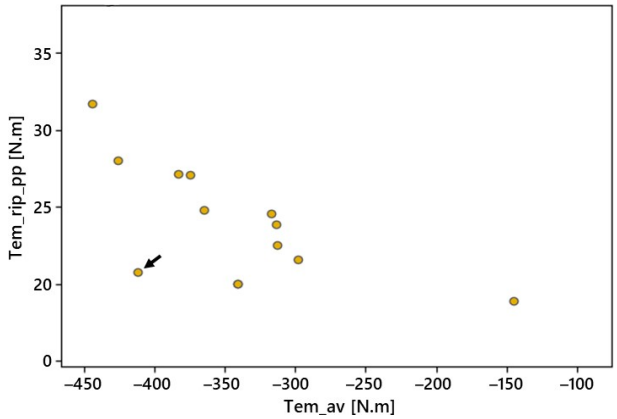

Fig. 8. Pareto front from which design A is selected.

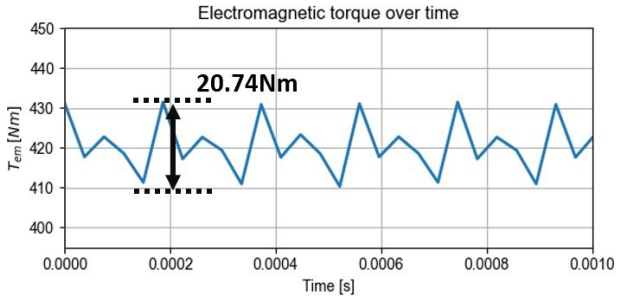

Fig. 9. Torque and torque ripples of design A..

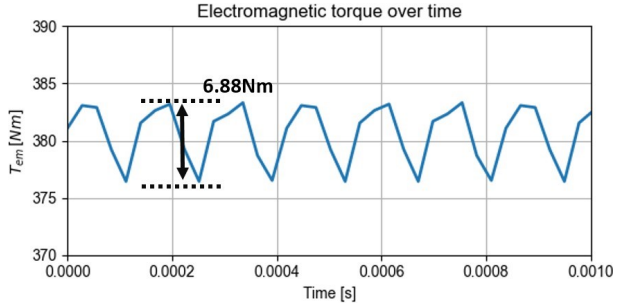

Fig. 10. Torque and torque ripples of design B.

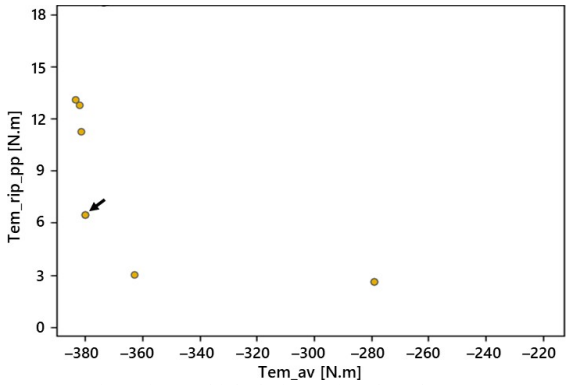

Fig. 11. Pareto front from which design B is selected.

In Fig. 12(a) and 12(b), the machine designs of optimized designs A and B, respectively, are shown to provide an understanding of changes in the design parameters. Compared to the initial design, a 0.13% increase in efficiency was observed with design A and a 4% decrease with design B.

To compare the performances, the torque speed characteristics of the initial design, optimized designs A and B, along with the Tesla baseline design are shown in Fig. 13. In this figure, it can be observed that with design A, there is a higher constant torque value as well as a slightly extended speed range. With design B, the constant torque region in reduced and at a lower value with a reduction in speed range compared to that of the initial design.

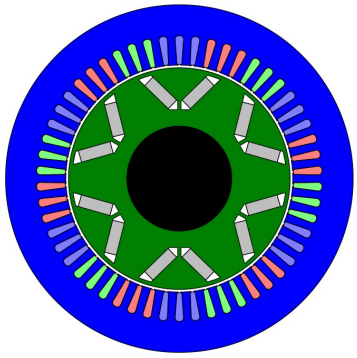

(a) Design A

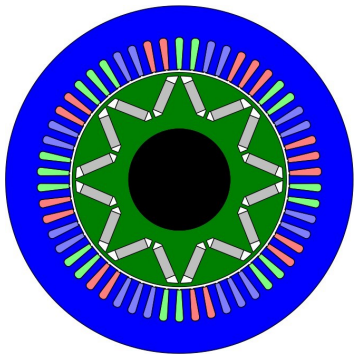

(b)Design B

Fig. 12. Optimized machine designs.

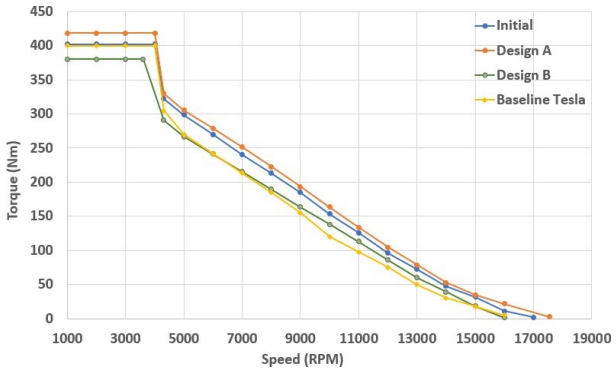

Fig. 13. Torque Speed characteristics.

B. Comparison

The choice of material, particularly that of the permanent magnets, plays an important role in the performance of the motor. Various neodymium magnet grades were explored and their effectt on the initial design and the optimized designs A and B are shown in Table IV. In addition to this, the cost per kilogram of these magnet grades were calculated based on the formula in [29] and thereby, the approximate magnet cost for the total magnet mass in these designs were also identified as shown in Table IV. The initial design has a total magnet mass of 2.08 kg and utilises the N40UH magnet grade, which costs

TABLE IV
EFFECT OF DIFFERENT MAGNET MATERIALS

Material	Initial			Magnet Cost	Optimised				Magnet Mass(kg)	Magnet Cost
	Torque (Nm)	Torque Ripples (Nm)	Power (kW)		Design	Torque (Nm)	Torque Ripples (Nm)	Power (kW)		
N30UH	371	23.56	148	$156	A	381	18.05	152	2.28	$171
					B	341	6.6	126	2.45	$183
N35UH	384	24.89	155	$183	A	390	19.54	158	2.28	$200
					B	354	6.65	134	2.45	$215
N40UH	402	30.57	167	$197	A	417	20.74	173	2.28	$216
					B	380	6.88	148	2.45	$232
N42UH	410	32.12	171	$214	A	425	20.85	175	2.28	$234
					B	389	7.17	154	2.45	$252

approximately $95/kg [30]. Out of these magnet grades, N42UH can be seen to increase the overall torque and power without a significant change in torque ripples for designs A and B.

To understand the performance of the optimal designs, their torque speed characteristics were obtained by varying the magnet grades, and this comparison has been shown in Fig. 14. It can be observed that design A with the N42UH magnet has the highest constant torque value and, as mentioned previously, an extended speed range. Design B on the other hand has a reduced speed range and constant torque region, and thus N30UH has the least constant torque value. Magnetic flux density distributions of designs A and B produced using Finite Element Magnetic Modelling (FEMM) software are shown in Fig. 15.

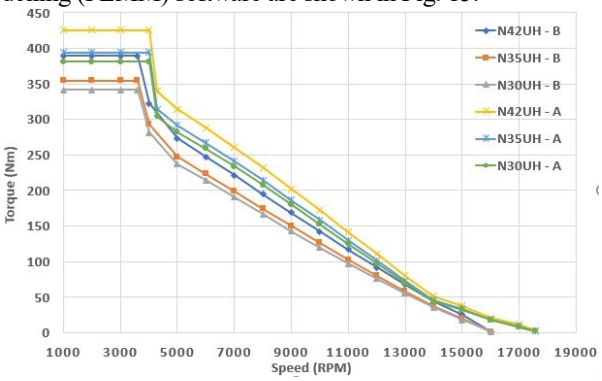

Fig. 14. Torque Speed characteristics of different magnet grades.

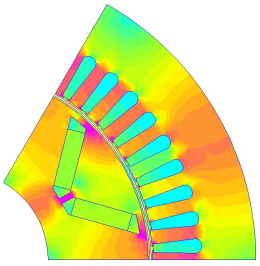

(a) Initial

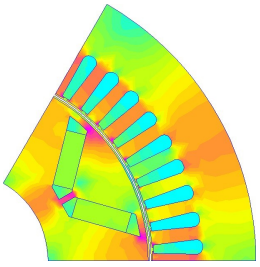

(b) Design A

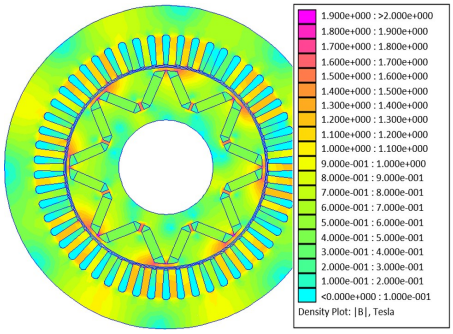

(c) Design B

Fig. 15. Magnetic field distribution of the initial and optimized designs.

IV. DISCUSSION

Following optimization, two designs A and B were identified as suitable solutions. Although torque and power are important objectives, the focus of this paper was on minimizing the torque ripples, as it could deteriorate the performance of the motor. On comparing their results, design A produced 20.74 Nm of torque ripples, which is less than the initial design but large enough to still pose unwanted threats to the motor performance. As discussed in the sensitivity analysis section, the torque ripples can be reduced with increase in pole number. Similarly, the decrease in magnet height and increase in stator teeth height aided this. Therefore, with design B, the reduction in torque ripples is significant which satisfied the main objective of this paper, although it was accompanied by a marginal decrease in the overall torque.

V. CONCLUSION

This paper presented the issue of cogging torque and its effect on the performance of interior permanent magnet motors. The influence of various design parameters on the overall torque and torque ripples of the designed motor were analyzed, and this enabled the identification of an appropriate starting point for the optimization process with the NSGA-II genetic algorithm. The optimization yielded two designs whose performances were compared in terms of the overall torque, torque ripples, and power. This demonstrated that the design B with increased pole number, stator diameter, teeth height, and reduced magnet length had a superior performance in terms of torque ripples, which was reduced by 77% compared to that of the initial design. While the initial design of the motor has an overall weight of approximately 35.75 kg, the two designs A

and B weigh 37 and 38 kg respectively. Therefore, it should be noted that the design B with the lowest torque ripples is also a heavier solution. Furthermore, analysis was extended to the performance of designs based on different magnet grades and their respective results were compared along with their material cost.

REFERENCES

[1] I. Aijaz, and A. Ahmad, "Electric Vehicles for Environmental Sustainability", *Smart Technologies for Energy and Environmental Sustainability*, 131–145, 2021. [Online]. Available: https://doi.org/10.1007/978-3-030-80702-3_8

[2] M. F. Torquato, K. Lakshmanan, and N. Narozanska *et al*, "Cascade Optimization of Battery Electric Vehicle Powertrains", *Procedia Computer Science*, pp. 592-601, Spet. 2021.

[3] D. J. Vogel, M. W. Toffel, and D.Post *et al*, "Environmental Federalism in the European Union and the United States", *SSRN Electronic Journal*, 2010. [Online]. Available: https://doi.org/10.2139/ssrn.1573698

[4] Y. Huang, C. Lei, and C. H. Liu *et al*, "A Review of Strategies for Mitigating Roadside Air Pollution in Urban Street Canyons", *Environmental Pollution*, 116971, 2021. [Online]. Available: https://doi.org/10.1016/j.envpol.2021.116971

[5] G. Conway, A. Joshi, and F. Leach *et al*, "A Review of Current and Future Powertrain Technologies and Trends in 2020", *Transportation Engineering*, *5*, 100080, 2021. [Online]. Available: https://doi.org/10.1016/j.treng.2021.100080

[6] A. Sheela, and A. Mohan, "Design of Permanent Magnet Synchronous Motor for Electric Vehicle Application Using Finite Element Analysis", *INTERNATIONAL JOURNAL of SCIENTIFIC and TECHNOLOGY RESEARCH*, vol. 9, no. 3, pp. 523–527, 2020.

[7] A. Dalcalı, E. Kurt, and E. Çelik *et al*, "Cogging Torque Minimization Using Skewed and Separated Magnet Geometries", *Journal of Polytechnic,* 2019. https://doi.org/10.2339/politeknik.552273

[8] P. Xu, K. Shi, and Y. Sun *et al*, "Effect of Pole Number and Slot Number on Performance of Dual Rotor Permanent Magnet Wind Power Generator Using Ferrite Magnets", *AIP Advances*, vol. 7, no. 5, pp. 056631, 2017.

[9] Q. Xu, J. Sun, and W. Wang *et al*, "Design Optimization of an Electric Variable Transmission for Hybrid Electric Vehicles. *Energies"*, vol. 11, no. 5*,* pp. 1118, 2018.

[10] M. Chaieb, S. Tounsi, and R. Neji, *et al*, "Optimum Geometry for Torque Ripple Minimization of Permanent Magnet Motor by the Finite Element Method", in *Proc. of MELECON 2008-the 14th IEEE Mediterranean Electrotechnical Conference*, Ajaccio, France, May 2008.

[11] R. Abdelmoula, B. Naourez, and M. Chaieb *et al* "Reducing torque ripples in permanent magnet synchronous motor", *Journal of Electrical Systems*, vol. 13, no. 3, pp. 528–542, 2017.

[12] Z. Q. Zhu, and D. Howe, "Influence of Design Parameters on Cogging Torque in Permanent Magnet Machines". *IEEE Transactions on Energy Conversion*, vol. 15, no. 4, pp. 407–412, 2000.

[13] M.-H. Hwang, H.-S. Lee, and H.-R. Cha, "Analysis of Torque Ripple and Cogging Torque Reduction in Electric Vehicle Traction Platform Applying Rotor Notched Design. *Energies*, vol. 11, no. 11, pp. 3053, 2018.

[14] Emrullah Aydin, Yingjie Li, and Ilhan Aydin *et al*, "Minimization of Torque Ripples of Interior Permanent Magnet Synchronous Motors by Particle Swarm Optimization Technique", in *Proc. of 2015 IEEE Transportation Electrification Conference and Expo (ITEC),* Dearborn, MI, USA, 2015.

[15] W. Q. Chu and Z. Q. Zhu, "Investigation of Torque Ripples in Permanent Magnet Synchronous Machines with Skewing". *IEEE Transactions on Magnetics*, vol. 49, no. 3, pp. 1211-1220, 2013.

[16] Alexandru-Ionel Constantin, Constantin Dumitru, and Emil Tudor *et al*, "Studies Related to the Optimization of an Interior Permanent Magnet Synchronous Machine Designed for the Electric Vehicles", in *Proc. of 2021 International Conference on Applied and Theoretical Electricity (ICATE),* Craiova, Romania, 2021.

[17] *Tesla Model 3 2018 Motor Analysis with Winding Diagram, Estore.Ricardo.Com.* [Online]. Available: https://estore.ricardo.com/en/2018-tesla-model-3-motor-report-with-winding-analysis—c-23-c-70-p-481.

[18] *Neodymium Magnets (NdFeB)*. (n.d.). Arnold Magnetic Technologies. [Online]. Available: https://www.arnoldmagnetics.com/products/neodymium-iron-boron-magnets/

[19] M. S. Toulabi, J. Salmon, and A. M. Knight, "Concentrated Winding IPM Synchronous Motor Design for Wide Field Weakening Applications", *IEEE Transactions on Industry Applications*, vol. 53, no. 3, pp. 1892–1900, 2017.

[20] P. Bonneel, Jean Le Besnerais, and R. Pile *et al*, "Pyleecan: an Open-Source Python Object-oriented Software for the Multiphysic Design Optimization of Electrical Machines", in *Proc. of 2018 XIII International Conference on Electrical Machines (ICEM),* Alexandroupoli, Greece, 2018.

[21] M. Norhisam, Ahmad Fikri Nazifah, and I. Aris, Hiroyuki Wakiwaka *et al*, "Effect of Magnet Size on Torque Characteristic of Three Phase Permanent Magnet Brushless DC Motor", *Student Conference on Research and Development,* 2010.

[22] C. Jędryczka, D. Danielczyk, and W. Szeląg, "Torque Ripple Minimization of the Permanent Magnet Synchronous Machine by Modulation of the Phase Currents", *Sensors*, vol. 20, no. 8, pp. 2406, 2020.

[23] K. Deb, A. Pratap, and S. Agarwal *et al*, "A Fast and Elitist Multiobjective Genetic Algorithm: NSGA-II", *IEEE Transactions on Evolutionary Computation*, vol. 6, no. 2, pp. 182–197, 2002.

[24] Raouf Benlamine, F. Dubas, and S. A. Randi *et al*, "Design by Optimization of an Axial-flux Permanent-Magnet Synchronous Motor Using Genetic Algorithms", in *Proc. of 2013 International Conference on Electrical Machines and Systems (ICEMS),* Busan, Korea (South), 2013.

[25] K. Deb. *Multi-objective Optimization Using Evolutionary Algorithms: an Introduction*, Springer, 2011, pp. 3-34.

[26] Fangwu Ma, Hongbin Yin, and Lulu Wei *et al*, "Design and Optimization of IPM Motor Considering Flux Weakening Capability and Vibration for Electric Vehicle Applications", *Sustainability*, vol. 10, no. 5, pp. 1533, 2018.

[27] Tao Deng, Chunsong Lin, and Junlin Luo *et al*, "NSGA-II Multi-objectives Optimization Algorithm for Energy Management Control of Hybrid Electric Vehicle", *Proceedings of the Institution of Mechanical Engineers, Part D: Journal of Automobile Engineering*, vol. 233, no. 4, pp. 1023–1034, 2019.

[28] J. Le Besnerais, V. Lanfranchi, and M. Hecquet *et al*, "Multiobjective Optimization of Induction Machines Including Mixed Variables and Noise Minimization", *IEEE Transactions on Magnetics*, vol. 44, no. 6, pp. 1102–1105, 2008.

[29] N. A.Bhuiyan, and A. McDonald, "Optimization of Offshore Direct Drive Wind Turbine Generators with Consideration of Permanent Magnet Grade and Temperature", *IEEE Transactions on Energy Conversion*, vol. 34, no. 2, pp. 1105–1114, 2019.

[30] A. Dalcali, "A Comparative Study of PM Synchronous Generator for Micro Hydropower Plants", *Balkan Journal of Electrical and Computer Engineering*, pp. 17-22, 2021.

Lavanya Balasubramanian received the B.Tech. degree in Electronics and Communication Engineering from the SRM University, Chennai, India, in 2017, and the M.Sc. degree in Robotics from the University of Sheffield, UK, in 2019. She is currently a Project Assistant with the Advanced Sustainable Manufacturing Technologies (ASTUTE2020) operation, Swansea University, UK. Her research interests include electric machines, electronics, industrial and healthcare robotics.

Nurul Azim Bhuiyan received the B.Sc. degree in Electrical and Electronic Engineering from the Ahsanullah University of Science and Technology, Dhaka, Bangladesh in 2007, M.Sc. degree in Sustainable Electrical Power from the Brunel University, London, UK in 2011 and Ph.D. degree in modelling, design and optimization of generators for large offshore wind turbine from the University of Strathclyde, Glasgow, UK in 2018. He is currently a Project Assistant with the Advanced Sustainable Manufacturing Technologies (ASTUTE2020) operation, Swansea University, UK.

Asad Javied has done his PhD in wireless communications signal processing from University of Surrey, UK and later worked in various roles in industry as well as in academia related to sensor data processing, electronic system design and machine learning. He is currently working as research scientist in the ASTUTE institute, Swansea.

Ashraf A. Fahmy received the BEng (Hons) in Electrical Engineering, 1992, the MSc with specialization in Flux Vector Control of Electric Machines, 1999, both from Helwan University, Cairo, Egypt, and the Ph.D. with specialization in Neuro-Fuzzy Control of Robotic Manipulators, 2005, from Cardiff University, UK. He has expertise in soft computing decision making, manufacturing systems, robotic manipulation, instrumentation, control systems, and electrical power generation. He is an Associate Professor at Helwan University, currently the Senior Technical Manager at ASTUTE in the Engineering College of Swansea University, and Freelancer HV Consultant at Shaker Consultancy Group. He is an Electrical Power and Machines drives' control engineer by education and worldwide experience, Robotics control engineer by research, and industrial manufacturing consultant by UK and worldwide experience.

Fawzi Belblidia received the BEng (Hons) from the Mechanical Department-Ecole Polytechnique Alger, Algeria in 1987, followed by the MSc in 1990 in the same institution, and the Ph.D. in 1999, in Swansea University, UK on subject related to fully integrated structural optimization modelling techniques. He currently holds a managing technical role with ASTUTE2020 operation in the College of Engineering, Swansea University overseeing a number of collaborative RD projects with local companies and deploying his expertise in Advance Material Technology and Computational Engineering Modelling. He was a research officer within the College of Engineering, Swansea University since 1999 supported by several research grants. He is a Chartered Engineer (CEng) and a Member of the Institution of Mechanical Engineers (MIMehE)

Johann Seinz received the Diplom-Ingenieur (FH) in Mechanical Engineering with specialization in Aerospace Engineering from the University of Applied Sciences Augsburg, Germany, in 1989, the BEng (Hons) from the University of Central Lancashire, UK, in 1989, the MSc in 1990 and the Ph.D. in 1994, both from Swansea University, UK. He holds a Personal Chair in the College of Engineering, Swansea University, where he is the Deputy Head of College and the Director of Innovation and Engagement. He is a Fellow of the Institution of Mechanical Engineers (FIMechE) and of the Royal Aeronautical Society (FRAeS), and a Member of the Institute of Mathematics and its Applications (MIMA). He is a Chartered Engineer (CEng) and a Chartered Mathematician (CMath). He is Editor-in-Chief of the International Journal "Applied Mathematical Modelling" as well as being on the editorial board of several other international journals.